

On the  $A$  dependence of nuclear structure functions

J. Dias de Deus\*

CERN, CH-1211 Geneva 23, Switzerland

M. Pimenta and J. Varela

Centro de Física da Matéria Condensada,  
Instituto Nacional de Investigação Científica,  
Av. Prof. Gama Pinto 2, 1699 Lisboa Codex, Portugal  
(Received 8 May 1984)

We show that clustering of nucleons, with confinement-size changes, naturally explains and accurately describes recent data on the  $A$  dependence of deep-inelastic nuclear cross sections. Predictions for gluon distributions in nuclei are given.

Very recently, an experimental study of the atomic-weight  $A$  dependence of the ratio

$$r_A(x) = \frac{1}{A} F_A(x) / \frac{1}{2} F_D(x) \tag{1}$$

in the  $0.09 \leq x \leq 0.9$  region,<sup>1</sup> where  $F_A(x)$  [ $F_D(x)$ ] is the nucleus- $A$  [deuterium] deep-inelastic electron-scattering cross section and  $x$  the Bjorken scaling variable, has shown that if  $r_A(x)$  is parametrized in the form

$$r_A(x) \approx A^{\alpha(x)}, \tag{2}$$

the function  $\alpha(x)$  has a highly nontrivial behavior (see the experimental points in Fig. 1). In fact, for  $x \approx 0.2$ ,  $\alpha(0.2) \approx 0$ ; for  $x \approx 0.65$ ,  $\alpha$  shows a minimum,  $\alpha(0.65) \approx -0.0045$ ; for  $x \geq 0.8$ ,  $\alpha$  increases very rapidly, becoming positive. This behavior, as emphasized in Ref. 1, will provide a test for theoretical models.

In this note we would like to show that models including clustering effects (kinematic and size effects) can naturally explain the observed  $A$  dependence of  $r_A(x)$ , i.e., the  $x$  dependence of  $\alpha(x)$ —see the curves in Fig. 1. We further show that a detailed description of  $r_A(x)$  for different nuclei can be achieved with the model of Ref. 2—see the fits in

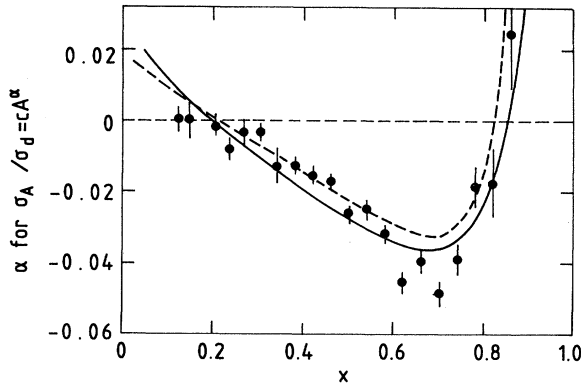


FIG. 1. The  $x$  dependence of the deep-inelastic cross-section ratios:  $r_A(x) = A^{\alpha(x)}$ . Solid curve, result from the fit to the eight nuclei of Ref. 1 with  $\lambda = 0.012$ . Dashed curve, simplified model, Eqs. (9) and (10), with not unreasonable values of the parameters,  $\beta_1 = 2$ ,  $\lambda = 0.02$ .

Fig. 2. Finally, Fig. 3 contains our predictions for the gluon distribution ratio  $r_{Fe}^G(x)$  and the corresponding parameter  $\alpha^G(x)$ .

Clustering of quarks, or nucleons, in nuclei changes parton distributions in two very distinct manners.<sup>2</sup> On the one hand, the momentum has to be shared by a larger number of constituents and this affects the fast-parton (valence-quark) distribution. In a  $(1-x_i)^{\beta_i}$  parametrization of the valence distribution,

$$F_A(x) \underset{x_i \geq 1/3i}{\sim} (1-x_i)^{\beta_i}, \tag{3}$$

where  $i$  is the average number of nucleons per cluster, always very close to 1, and  $x_i = x/i$  is the parton momentum fraction relative to the cluster momentum, the usual counting-rule arguments give

$$\beta_i = \beta_1 + 6(i-1). \tag{4}$$

As  $\beta_i > \beta_1$  there is a suppression of the distribution in the intermediate- $x$  region. As  $x_i < x$  there is an increase of the ratio (1) in the  $x \rightarrow 1$  region. The clustering of  $i$  nucleons, on the other hand, gives rise to a large effective confinement-size parameter  $R_i$ :

$$R_i = R_1 i^{1/3}. \tag{5}$$

This means that the perturbative  $Q^2$  evolution “starts” earlier in nuclei, with the consequence that, for a given  $Q^2$ , there are more sea quarks and gluons per nucleon in nuclei than in the nucleon.<sup>3</sup>

It is clear that using (3) and (4) for the fast-parton distribution and (5) for the hadronic scale in the QCD  $Q^2$  evolution, the general features of the  $x$  dependence of the ratio (1) (Ref. 4) can be easily obtained. In Ref. 2, an overall discussion of these ideas was given and fits to the existing data were presented.

In order to make comparisons with experiment,<sup>1</sup> we need now a relation between  $i$ , or  $R_i$ , and  $A$ . There are several proposals<sup>3,5,6</sup> all in the same spirit, relating  $R_i$  to the multinucleon overlap probability inside the nucleus. Here, we simply write

$$i \approx A^\lambda, \tag{6}$$

with  $\lambda$  being a free parameter.

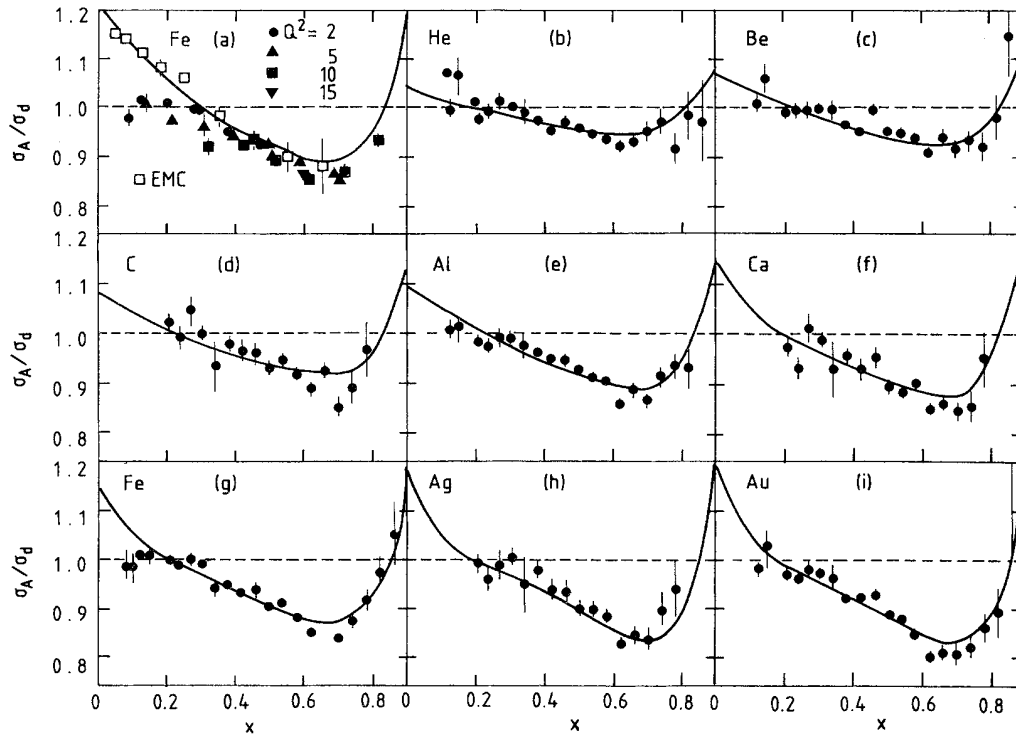


FIG. 2. The ratio  $r_A(x) = \sigma_A/\sigma_D$  of deep-inelastic cross sections. Data: the solid circles are from Ref. 1 and the open squares from the European Muon Collaboration (EMC) (Ref. 4). (a) Fit to the EMC data from Ref. 2. (b)–(i) Fit to Ref. 1 data, giving  $\lambda = 0.012$ .

We present now the results of our fits to the data of Ref. 1 (Figs. 1 and 2) with the model of Ref. 2. In the model, conventional parametrizations of valence sea and gluon distributions were used. As input, we took the deuteron parton-distribution parameters, from fits to deuteron data, of Table 1 of Ref. 2, with  $R_1 = R_D = 4.3 \text{ GeV}^{-1}$  and  $i_D = 1$ . The constraints (4), (5), and (6) were imposed<sup>7</sup> and  $\lambda$  was left as the only parameter to adjust in the simultaneous fit to the eight nuclear-structure-function ratios  $r_A(x)$  (Ref. 1). For the parameter  $\lambda$  we obtained  $\lambda = 0.012$ .

Equation (6) was found to be very well satisfied and we checked, by comparing the obtained fits, using (6) and  $\lambda$ , with independent fits for each nucleus, that the values of  $i$  determined in the two ways agree very closely. There are two exceptions, D, which lies below (6), and He, which lies slightly above. This means that the density of D has a value below the average density and the density of He has a value above.

As the knowledge of gluon distributions is of considerable theoretical and experimental interest, we present in Fig. 3 our results for the ratio  $r_A^G(x)$  of gluon structure functions of Fe and D [Fig. 3(a)], and for the gluon-distribution parameter  $\alpha^G(x)$ , defined analogously to  $\alpha(x)$  [Fig. 3(b)]. The deviations of  $r_A^G(x)$  from 1 and of  $\alpha^G(x)$  from 0 are more pronounced than the corresponding deviations of  $r_A(x)$  and  $\alpha(x)$ , also shown in Fig. 3, and the minima of  $r_A^G(x)$  and  $\alpha^G(x)$  occur at a larger value of  $x$ ,  $x \approx 0.8$ . Our parametrizations of gluon distributions are presumably not very reliable, as they are fixed from deep-inelastic scattering data only. However, the perturbative QCD evolution equations, with different size factors, will necessarily generate the large effects in  $r_A^G$  (and  $\alpha^G$ ) seen in Fig. 3, as one re-

quires at the same time an increase in the number of gluons keeping roughly constant the fraction of momentum carried by them.

We finally would like to argue that the success of our fits is not accidental: any model including cluster effects (kinematic and confinement-size effects) is able to describe, approximately at least, the deep-inelastic scattering data. We consider then the toy model of Ref. 6, which mimics the model of Ref. 2 and has the advantage of allowing for a simple analytic treatment. We write for the nucleus- $A$  structure function

$$\frac{1}{A} F_A(x) \equiv \frac{1}{i} F_i(x) = \frac{f}{i} (\beta_i + 1) (1 - x/i)^{\beta_i}, \quad (7)$$

where  $f$  is a constant. Equation (7) shows the correct large- $x_i$  behavior, (3) and (4), the relative increase in the number of sea quarks,

$$\frac{1}{i} F_i(0)/F_1(0) > 1,$$

and gives a constant,  $A$ -independent, fraction of the momentum carried by the gluons,

$$\langle G \rangle = 1 - \langle V \rangle - \langle S \rangle = 1 - f.$$

This last feature, related to the QCD evolution equations, corresponds to the situation occurring in the model of Ref. 2, for values  $Q^2 \geq 2 \text{ GeV}^2$ , as the fraction of momentum taken by gluons very quickly reaches a value close to the asymptotic limit and becomes weakly dependent on  $Q^2$  and  $A$ .

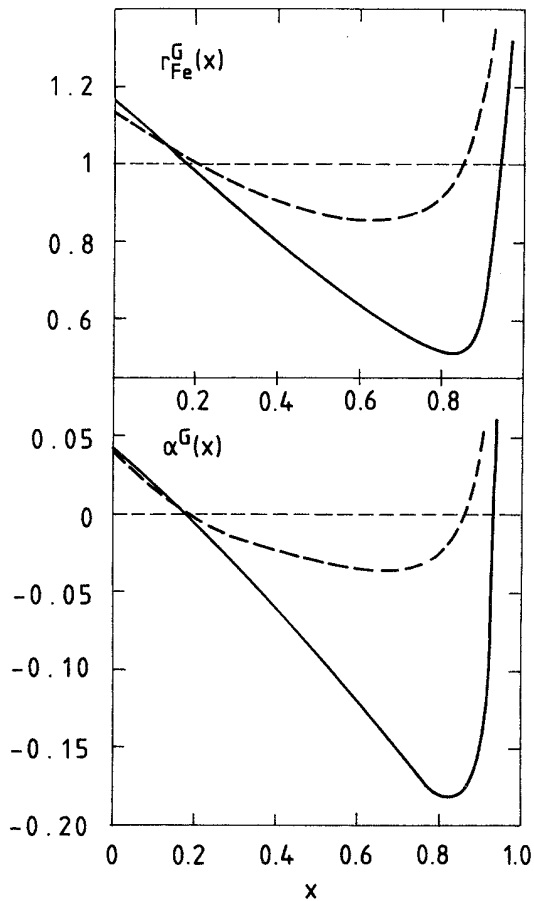


FIG. 3. Gluon structure-function ratio  $r_A^G(x)$  and the parameter  $\alpha^G(x)$  (solid curve). For comparison we show  $r_A(x)$  and  $\alpha(x)$  (dashed curve).  $Q^2 = 10 \text{ GeV}^2$  and  $\lambda = 0.012$ . (a) The ratio  $r_A^G(x)$  for Fe/D. (b) The  $x$  dependence of  $\alpha^G(x)$ .

Combining (2) and (6) we can write

$$r_A(x) \equiv r_i(x) = i^{\rho(x)}, \quad (8)$$

with

$$\alpha(x) = \lambda \rho(x). \quad (9)$$

The function  $\rho(x)$  can now be computed from (8), (1), and (7). Having in mind that because of the saturation of nuclear matter density in nuclei at a low value,  $i$  is always very close to 1, we obtain, making use of (4),

$$\rho(x) \equiv \frac{i}{r_i} \frac{dr_i}{di} \approx \frac{5 - \beta_i}{\beta_i + 1} + \beta_i \frac{x}{1 - x} + 6 \ln(1 - x). \quad (10)$$

The function  $\rho(x)$  [Eq. (10)] shows two zeros and a minimum in the  $0 < x < 1$  region. The minimum occurs at

$$x_{\min} = 1 - \beta_i/6, \quad (11)$$

exactly at the same point as the minimum of  $r_A(x)$ , Eqs. (1) and (7). As  $\rho(x)$  is trivially related to  $\alpha(x)$  by (9) it is obvious that (10) has the correct features observed for  $\alpha(x)$  in Ref. 1. A curve for  $\alpha(x)$ , using (10) and (9), is shown (dashed curve) in Fig. 1.

We would like to stress that the reason we are able to describe the turnover of  $\alpha(x)$  at  $x \approx 0.6$  and the rise as  $x \rightarrow 1$  is related to the kinematic clustering factor  $x/i$  in (3). The contribution from this factor is the term  $\sim x/(1-x)$  in (10). It is this term that causes the turnover and the rise as  $x \rightarrow 1$  in  $\alpha(x)$ . Models containing size effects only<sup>3</sup> may describe data on  $r_A(x)$  and  $\alpha(x)$  up to  $x \approx 0.6$  but necessarily miss the larger- $x$  region.

One of us (J. Dias de Deus) would like to thank E. Gathuler for conversations and the CERN-TH Division for the kind hospitality.

\*On leave of absence from Centro de Física da Matéria Condensada, Instituto Nacional de Investigação Científica, Av. Prof. Gama Pinto 2, 1699 Lisboa Codex, Portugal.

<sup>1</sup>R. G. Arnold *et al.*, Phys. Rev. Lett. **52**, 727 (1984).

<sup>2</sup>J. Dias de Deus, M. Pimenta, and J. Varela, Centro de Física da Matéria Condensada Report No. CFMC E-1/84 (unpublished).

<sup>3</sup>F. Close, R. Roberts, and G. Ross, Phys. Lett. **129B**, 346 (1983); F. Close, R. Jaffe, R. Roberts, and G. Ross, *ibid.* **134B**, 449 (1984).

<sup>4</sup>J. J. Aubert *et al.*, Phys. Lett. **123B**, 275 (1983); A. Bodek *et al.*,

Phys. Rev. Lett. **50**, 1431 (1983); *ibid.* **51**, 534 (1983).

<sup>5</sup>J. Dias de Deus, Max-Planck-Institute Report No. MPI-PAE/PTH G1/83 (revised), 1983 (unpublished).

<sup>6</sup>H. J. Pirner and J. P. Vary, Phys. Rev. Lett. **46**, 1379 (1981).

<sup>7</sup>In Ref. 2, constraints (4) and (5) were not used and  $\beta_i$  and  $R_i$  were free parameters. In practice, constraint (4) is always fairly well satisfied. Constraint (5) on  $R_i$  has to be used here because  $R_i$  mostly affects small  $x$ , where there are few points and at small values of  $Q^2$ . In fact, in the fits, we have only used the points with  $x > 0.2$ .